Vacuum 145 (2017) 272–277

Contents lists available at ScienceDirect

Vacuum

journal homepage: www.elsevier.com/locate/vacuum

Anharmonic effects of gold in extended X-ray absorption fine structure

Nguyen Ba Duc [a], Vu Quang Tho [a], Nguyen Van Hung [b], Doan Quoc Khoa [c, *], Ho Khac Hieu [c, **]

[a] Tan Trao University, Tuyen Quang, Viet Nam
[b] VNU University of Science, Ha Noi, Viet Nam
[c] Duy Tan University, Da Nang, Viet Nam

ARTICLE INFO

Article history:
Received 12 June 2017
Received in revised form
27 August 2017
Accepted 6 September 2017
Available online 7 September 2017

Keywords:
Anharmonicity
Gold
EXAFS
Cumulant
Debye-waller factor

ABSTRACT

The anharmonic effects of gold in extended X-ray absorption fine structure (EXAFS) have been investigated through the consideration of the first four EXAFS cumulants up to temperature 800 K within the anharmonic correlated Debye model. The interatomic potential between two intermediate atoms has been described by the second-moment approximation to the tight-binding model and its parameters were determined from first-principles calculations. Our results of the first four EXAFS cumulants and anharmonic effective potential are compared with those of experiments showing the good and reasonable agreements. We have shown in detail that the anharmonicity contributions of the thermal vibration of atoms are important to EXAFS cumulants at high temperature.

1. Introduction

The extended X-ray absorption fine structure (EXAFS) spectroscopy is a powerful technique for investigating local structures of crystalline as well as amorphous materials [1,2]. It provides apparently different structural information such as bond distances, coordination number and geometry at various high temperature due to anharmonicity [3,4]. This technique can be used independently or in coordination with X-ray crystallography or nuclear magnetic resonance spectroscopy [1]. The formalism for including anharmonic effects in EXAFS is often written on the basis of the cumulant expansion approach as [5,6].

$$\chi(k) = \frac{F(k)}{kR^2} e^{-2R/\lambda(k)} \mathrm{Im}\left\{ e^{i\varphi(k)} \exp\left[2ikR + \sum_n \frac{(2ik)^n}{n!} C_n \right] \right\}, \quad (1)$$

where k and λ are, respectively, the wave number and mean free path of emitted photoelectrons, $F(k)$ is the real atomic backscattering amplitude, $\varphi(k)$ is net phase shift, the thermal average distance $R = \langle r \rangle$ with r is the instantaneous bond length between absorbing and backscattering atoms, and C_n $(n = 1, 2, 3, \ldots)$ are the EXAFS cumulants. The cumulant method allows the characterization of the first coordination shell in terms of parameters which describe the distance distributions as the first cumulant C_1 is the mean value which describes the net thermal expansion or disorder; the second cumulant C_2 is the variance which characterizes the Debye-Waller factor [7,8]; the third cumulant C_3 measures the distribution asymmetry which describes the asymmetry of the pair distribution function; and the fourth cumulant C_4 measures the flatness of distribution function and gives the anharmonic contribution to EXAFS amplitude [9,10].

There are many methods that have been developed in order to study the temperature dependence of EXAFS cumulants such as path-integral effective-potential theory [11], statistical moment method [12], Debye model [13] and Einstein model [14]. A simple connection between EXAFS cumulants and pair interaction potential has been obtained for a cluster of atoms using the correlated Einstein model [14] and the first-order thermodynamic perturbation theory [15,16]. However, to the best of our knowledge, no theoretical calculations has been done to predict the temperature

* Corresponding author.
** Corresponding author.
E-mail addresses: khoa_dq@qtttc.edu.vn (D.Q. Khoa), hieuhk@duytan.edu.vn (H.K. Hieu).

http://dx.doi.org/10.1016/j.vacuum.2017.09.009
0042-207X/

effects on EXAFS cumulants of gold metal. One of the reason is that the Morse potential, which is frequently used in Einstein and Debye model [17,18], is not suitable to describe the complex atomic interaction of gold metal. It requires the more accurate interatomic interaction form for metallic systems such as the many body embedded-atom potentials [19], Finnis–Sinclair [20], Rosato–Guillopé–Legrand [21], and Sutton–Chen [22,23] types. Experimentally, several EXAFS measurements for gold were performed at ambient pressure [24,25] and under pressures up to 14 GPa using large volume high-pressure devices [26]. And then the cumulants were derived by the best fitting of experimental spectra to the simulated spectra built up using theoretical phases and amplitudes provided by the FEFF code [25,27].

The purpose of this work is to investigate the anharmonicity contributions to the EXAFS cumulants up to fourth order of gold metal. Anharmonic correlated Debye model (ACDM) [18] has been applied for gold crystal on the basis of the interatomic potential which has been derived by the second-moment approximation (SMA) to the tight-binding (TB) model [28]. The numerical results have been carried out and compared to other results and experimental values.

2. Theory

First of all, we summarize the results of EXAFS cumulants which were derived based on the correlated Debye model [13]. In solid-state physics, for the crystal with N atoms, the Debye model assumes a homogeneous system with a constant speed of sound c, the same linear dispersion relation $\omega = c.k$, and the density of states is quadratic as it is in the long wavelength limit. The maximum phonon frequency ω_D is so-called the Debye frequency, $\theta_D = \frac{\hbar\omega_D}{k_B}$ (k_B is the Boltzmann constant, $\hbar$ is the reduced Planck constant) is the Debye temperature above which all modes begin to be excited and below which modes begin to be "frozen out", $c = \omega_D/k_D$ is the Debye approximation for the speed of sound and $k_D = (6\pi^2 N/V)^{1/3}$ is a measure of the inverse inter-particle spacing [29].

The correlated Debye model in EXAFS may be defined as an oscillation of a pair of atoms with masses M_1 and M_2 (e.g., absorber and backscatterer) in a given system. This model has been used efficiently to estimate the temperature-dependent EXAFS cumulants [30]. The ACDM is a further development of the correlated Debye model based on the anharmonic effective interaction potential which is given by Ref. [18].

$$V_{eff}(x) = V(x) + \sum_{j\neq i} V\left(\frac{\mu}{M_i} x\widehat{\mathbf{R}}_{12}.\widehat{\mathbf{R}}_{ij}\right) \cong \frac{1}{2}k_{eff}x^2 + k_3x^3 + k_4x^4 + \cdots \widehat{\mathbf{R}} = \frac{\mathbf{R}}{|\mathbf{R}|}. \tag{2}$$

here the oscillation of absorber and backscatterer is influenced by their neighbors given by the last term in the left-hand side of Eq. (2), where the sum i is over absorber ($i = 1$) and backscatterer ($i = 2$), and the sum j is over all their nearest neighbors, excluding the absorber and backscatterer themselves. The latter contributions are described by the term $V(x)$. And k_{eff} is the effective force constant, k_3 and k_4 are, respectively, the cubic and quartic parameters giving an asymmetry in the pair distribution function due to anharmonicity and $x = r - r_0$ is the deviation of instantaneous bond length between the two intermediate atoms from equilibrium.

For the case of vibration between absorber and backscattering atoms and using the interatomic effective potential, the dispersion relation is expressed as [31].

$$\omega(q) = 2\sqrt{\frac{k_{eff}}{M}}\left|\sin\left(\frac{qa}{2}\right)\right|,\ |q| \leq \frac{\pi}{a}, \tag{3}$$

where q is the phonon wave number, M is the mass of composite atoms.

Applying for face-centered cubic crystals, the anharmonic interatomic effective potential in the present ACDM has the form as

$$V_{eff}(x) = V(x) + 2V\left(\frac{x}{2}\right) + 8V\left(-\frac{x}{4}\right) + 8V\left(\frac{x}{4}\right). \tag{4}$$

In this work, the interaction between metallic gold atoms is assumed, and could be described by an empirical many-body potential, derived in analogy of the TB-SMA model which is written as [32].

$$V(r) = V^B(r) + V^R(r), \tag{5}$$

where $V^B_{eff}(x)$ represents the band-structure term which has a many-body character due to its square root form as

$$V^B(r) = -\sqrt{\xi^2 e^{-2q[(r/r_0)-1]}}, \tag{6}$$

and $V^R(r)$ is a pair-potential repulsive term (Born-Mayer type),

$$V^R(r) = Ae^{-p[(r/r_0)-1]}. \tag{7}$$

It should be noted that, the TB-SMA potential takes into account the essential band character of the metallic bond: the band-structure term is proportional to the effective width of the electronic band and the repulsive pair-potential term, which incorporates the non-band-structure parts, includes electrostatic interactions [28]. The potential parameters have typically been determined by fitting to experimental data of cohesive energy, lattice constant, bulk modulus, and elastic constants of the system.

From the derived effective force constant, we obtain the force constants k_{eff}, k_3 and k_4 in terms of TB-SMA potential parameters and then the Debye frequency ω_D and Debye temperature θ_D as

$$\omega_D = 2\sqrt{\frac{k_{eff}}{M}};\ \theta_D = \frac{\hbar\omega_D}{k_B}. \tag{10}$$

Usually, anharmonic EXAFS analysis deals with the cumulants up to the fourth order which are related to the moments of the distribution function. The first four EXAFS cumulants within the ACDM have been recently derived by Hung et al. [18]. The first EXAFS cumulant describes the net thermal expansion or disorder in EXAFS theory. It was derived as

$$C_1 = \langle r - r_0\rangle = \frac{3\hbar a k_3}{2\pi k_{eff}^2}\int_0^{\pi/a} \omega(q)\frac{1+Z(q)}{1-Z(q)}dq. \tag{11}$$

To a good approximation, the second cumulant C_2 corresponds to the parallel mean-square relative displacement (MSRD) characterizing Debye-Waller factor which has the form as

$$C_2 = \left\langle (r - r_0 - C_1)^2 \right\rangle = -\frac{\hbar a}{2\pi k_{eff}} \int_0^{\pi/a} \omega(q) \frac{1 + Z(q)}{1 - Z(q)} dq$$
$$= -\sigma_0^2 \int_0^{\pi/a} \omega(q) \frac{1 + Z(q)}{1 - Z(q)} dq,$$

where $Z(q) = \exp[\beta\hbar\omega(q)]$, $\beta = 1/k_B T$ and$\sigma_o^2 = \frac{\hbar a}{2\pi k_{eff}}$ is the zero-point contributions to the second cumulant C_2.

The third cumulant describes the asymmetry of the pair distribution function in EXAFS theory and contributes to the phase shift of EXAFS spectroscopy. It has the following form

$$C_3 = \left\langle (r - r_0 - C_1)^3 \right\rangle = \frac{3\hbar^2 a^2 k_3}{4\pi^2 k_{eff}^3} \int_0^{\pi/a} dq_1 \int_{-\pi/a}^{\pi/a - q_1} F(q_1, q_2) dq_2$$

$$F(q_1, q_2) = \frac{\omega(q_1)\omega(q_2)\omega(q_1 + q_2)}{\omega(q_1) + \omega(q_2) + \omega(q_1 + q_2)}$$
$$\times \left\{ 1 + 6 \frac{\omega(q_1) + \omega(q_2)}{\omega(q_1) + \omega(q_2) - \omega(q_1 + q_2)} \frac{Z(q_1).Z(q_2) - Z(q_1 + q_2)}{[Z(q_1) - 1] \cdot [Z(q_2) - 1][Z(q_1 + q_2) - 1]} \right\}.$$

The fourth cumulant measures the flatness of distribution function and gives the anharmonic contribution to EXAFS amplitude. It has been derived and given by

$$C_4 = \left\langle (r - r_0 - C_1)^4 \right\rangle$$
$$= \frac{9\hbar^3 a^3 k_4}{4\pi^3 k_{eff}^4} \int_0^{\pi/a} dq_1 \int_0^{\pi/a - q_1} dq_2 \int_{-\pi/a}^{\pi/a - (q_1 + q_2)} G(q_1, q_2, q_3) dq_3$$

$$G(q_1, q_2, q_3) = \frac{\omega(q_1)\omega(q_2)\omega(q_3)\omega(q_4)}{\omega(q_1) + \omega(q_2) + \omega(q_3) + \omega(q_4)}$$
$$\times \left\{ \begin{array}{l} 1 + 8 \frac{\omega(q_1) + \omega(q_2) + \omega(q_3)}{\omega(q_1) + \omega(q_2) + \omega(q_3) - \omega(q_4)} \frac{Z(q_1) \cdot Z(q_2) \cdot Z(q_3) - Z(q_4)}{[Z(q_1) - 1] \cdot [Z(q_2) - 1][Z(q_3) - 1][Z(q_4) - 1]} + \\ +6 \frac{\omega(q_3) + \omega(q_4)}{\omega(q_1) + \omega(q_2) - \omega(q_3) - \omega(q_4)} \frac{Z(q_1).Z(q_2) - Z(q_3) \cdot Z(q_4)}{[Z(q_1) - 1] \cdot [Z(q_2) - 1][Z(q_3) - 1][Z(q_4) - 1]} \end{array} \right\}$$

with $q_4 = -(q_1 + q_2 + q_3)$.

3. Results and discussion

In this section, the expressions derived in the previous section is applied to numerically determine the first four EXAFS cumulants of gold metal. The TB-SMA potential parameters determined from first-principles calculations for gold bulk material are respectively $\xi = 1.8241$ eV, $A = 0.2145$ eV, $q = 4.3769$, $p = 10.8842$ and $r_0 = 2.8652$ Å [32]. Using these parameters, we derive the three force constants as follows $k_{eff} = 3.06$ eV/Å^2, $k_3 = -1.58$ eV/Å^3, and $k_4 = 1.79$ eV/Å^4. The second order effective force constant in our calculations $k_{eff} = 3.06$ eV/Å$^2 \approx 48.9$ N/m^2 is in reasonable agreement with those of estimations from the experimental phonon dispersion curves $k_{eff} = 39.9$ N/m$^2 \approx 2.49$ eV/Å^2[33], and from the experimental values of C_2 and C_3 in EXAFS measurements $k_{eff} = 3.80$ eV/Å$^2 = 60.8$ N/m^2[26]. Furthermore, using this effective force constant, we derive the Debye temperature of gold metal as $\theta_D = 186$ K. Our Debye temperature calculation is consistent with the one determined by fitting the experimental EXAFS oscillations $\theta_D = 180 \pm 4$ K performed by Comaschi et al. [25]. Especially, previous works also reported the value for the Debye temperature of gold bulk ranging from 165 K at low temperature to nearly 190±4 K at high temperature [34,35].

Our derived force constants were used for calculation of the anharmonic effective potential V_{eff} as a function of bond length deviation $x = r - r_0$ as shown in Fig. 1. The effective potentials derived by Okube et al. [26] (under pressure 0.1 MPa) and Comaschi et al. [25] have also been displayed for comparison. As observed in Fig. 1, there is a small difference between our effective potential and Okube et al.' one that can be explained by the narrow of potential width under pressure 0.1 MPa in Okube et al. measurements. The discrepancy of Comaschi et al.' result at the right hand-side of Fig. 1 could origin from the smaller force constant k_{eff} and the difference of the anharmonic effective force constant k_3. The values of k_3 in the present work, Okube et al. and Comaschi et al. determinations are -1.58 eV/Å^3,-1.27 eV/Å^3,and -1.94 eV/Å^3, respectively. Furthermore, there is the lack of the fourth order effective force constant k_4 in Comaschi et al.' and Okube et al.' works.

In Fig. 2, we show the thermal behavior of the first shell interatomic distance of the gold calculated by using the ACDM with the TB-SMA interaction potential. The inset figure is the interatomic distance difference ΔC_1, relative to the $T = 20$ K spectrum. Our results (solid lines) are compared with those of experimental

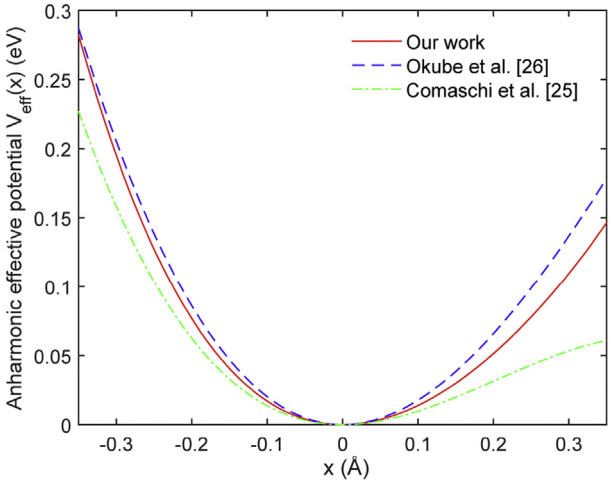

Fig. 1. Anharmonic effective potential of gold.

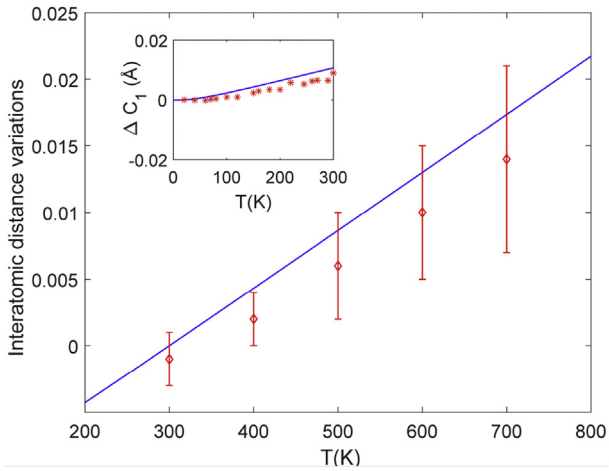

Fig. 2. Temperature-dependent interatomic distances of gold. Our calculations (solid lines) are presented in comparison to experimental data [24,25].

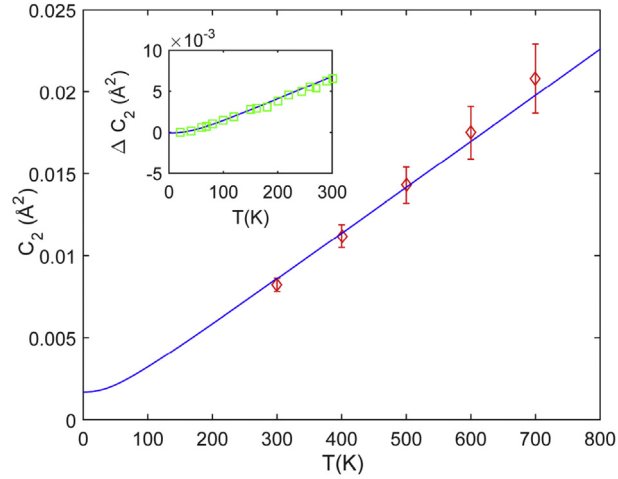

Fig. 3. Temperature dependence of the second cumulant C_2 of gold. Experimental data of C_2 [24] and the difference $\Delta C_2 = C_2(T) - C_2(20\,\mathrm{K})$[25] are shown for comparison.

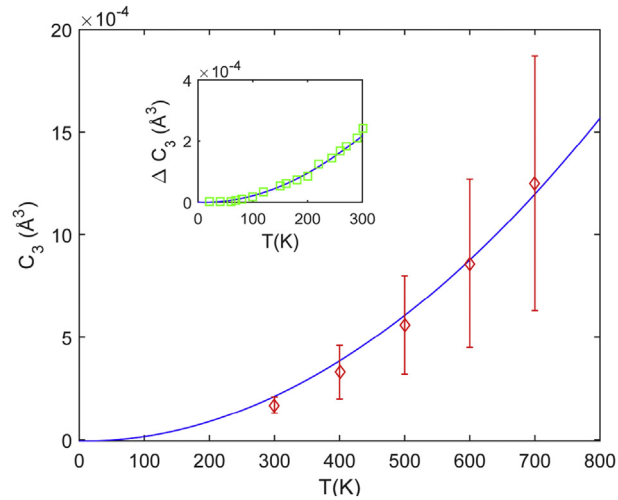

Fig. 4. Temperature dependence of the third cumulant C_3 of gold. Theoretical calculations (solid lines) are presented along with the experimental data of C_3 [24] and $\Delta C_3 = C_3(T) - C_3(20\,\mathrm{K})$[25].

measurements [24,25]. As observed in Fig. 2 that theoretical values are in reasonable agreement with the experimental measurements up to 800 K. The rapid increasing in the interatomic distances at high temperature indicates the stronger anharmonicity contribution of the thermal lattice vibration.

Fig. 3 reports the temperature dependence of the second cumulant C_2 and the difference $\Delta C_2 = C_2(T) - C_2(20\,\mathrm{K})$ (in 10^{-2} Å^2) between the second cumulant C_2 at temperature T and 20 K for the first-shell distances of Au metal in comparison to those of experimental results [24,25]. As seen in Fig. 3 that the good agreement between theoretical calculations and experimental measurements is found and the second cumulant increases rapidly with the increasing of temperature. The rapid increasing in the second cumulant C_2 also indicates the contributions of thermal lattice vibrations are important at high temperature. It means that the present ACDM formalism takes into account the quantum-mechanical zero-point vibrations as well as the anharmonicity and enables us to calculate the cumulants of crystals for a wide temperature range. Furthermore, it should be noted that the second cumulant C_2 corresponds to the parallel MSRD characterizing the EXAFS Debye-Waller factor that effects on the amplitudes of EXAFS oscillations. This factor is sensitive to both the structural and thermal disorder. The contribution of thermal disorder provides information on the effective bond stretching force constant between absorber-backscatterer pair corresponding to the dynamical properties of them.

In Fig. 4, we present the temperature dependence of the third cumulant C_3 obtained from the current ACDM approach up to 800 K together with the experimental data measured by Newville [24]. The inset figure is the relative values of the third cumulant $\Delta C_3 = C_3(T) - C_3(20\,\mathrm{K})$ up to 300 K. The experimental data of Comaschi et al. [25] are also displayed for comparison. Below 100 K the values of the third cumulant are very small but different from zero due to the zero point vibration contributions (a quantum effect). When temperature increases, the third cumulant grows progressively, showing an anharmonic contribution of thermal vibrations to C_3 at high temperature. It makes the deviation of the effective distribution from a Gaussian approximation. As observed in this figure we can see that our theoretical calculations of C_3 coincide with experimental data up to 800 K.

Here, it should be noted that, in EXAFS theory, the cumulant ratio $C_1.C_2/C_3$ is often considered as a criterion for cumulant study [17]. This ratio is used to identify the temperature threshold above

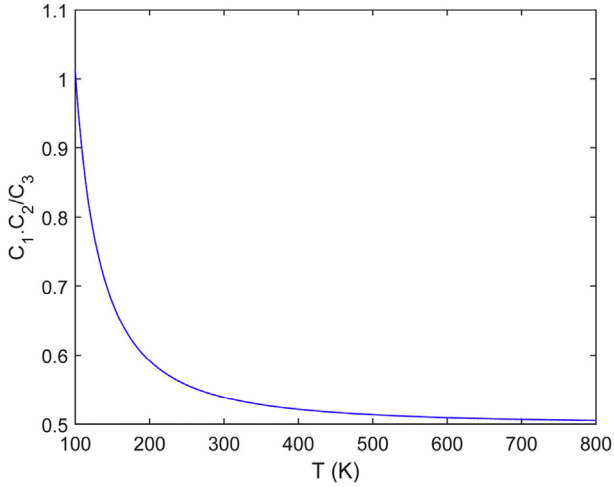

Fig. 5. Temperature dependence of cumulant ratio $C_1.C_2/C_3$ of gold.

which the cumulant ratio gradually approaches to the constant value of 1/2 so that the classical limit is suitable. In Fig. 5, we show the temperature dependence of the cumulant ratio $C_1.C_2/C_3$ of gold metal calculated using the present ACDM approach. The threshold temperature deduced from this work is about 500 K. The quantum theory is applicable for any temperature, but reduces to the classical limit at temperature higher than 500 K. Below 500 K the classical calculations lose validity.

The temperature dependence of the fourth cumulant C_4 of gold is shown in Fig. 6. As it can be seen from this figure, our results are in good agreement with experimental measurements performed by Newville [24]. The fourth cumulant C_4 is weakly sensitive to the temperature and then gives a small contribution to the amplitude to the EXAFS oscillations, e.g., it is less than 5% with wave number $k = 5$ Å^{-1}. Usually, this quantity and higher order cumulants can be neglected in EXAFS analysis.

4. Conclusions

In this work, the anharmonic effects of gold in EXAFS have been considered based on the investigation of EXAFS cumulant within the ACDM approach. The TB-SMA potential has been used to numerically calculate the first four EXAFS cumulants up to 800 K. Our calculations have shown that the anharmonicity contributions of thermal lattice vibrations are important to the first, second and third cumulants, especially at high temperature. This approach could be used to verify as well as analyze the future high-temperature EXAFS experiments. It could also be extended to study thermodynamic properties including anharmonicity of alloys in EXAFS theory in the near future.

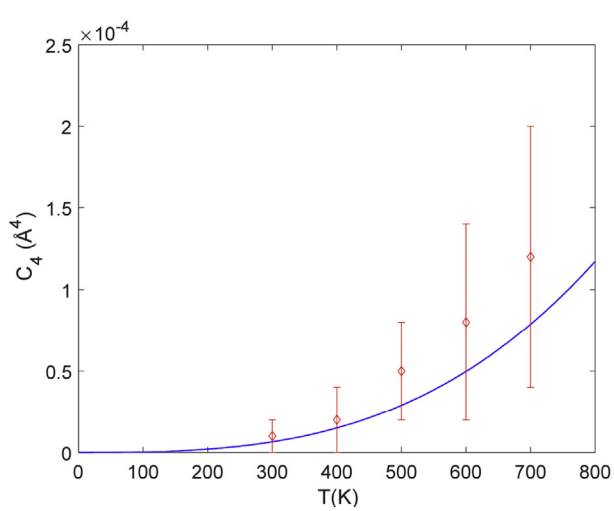

Fig. 6. Temperature dependence of the fourth cumulant C_4 of gold. Newville's experimental data of C_4 are also displayed for comparison [24].

Acknowledgements

This research is funded by the Tuyen Quang province under grant number ĐT.11-2016.

References

[1] O.M. Ozkendir, A. Yuzer, Influence of erbium substitution on the crystal and electronic properties of $FeBO_3$ oxide, Vacuum 141 (2017) 222–229, http://dx.doi.org/10.1016/j.vacuum.2017.04.021.
[2] W. Olovsson, B. Alling, M. Magnuson, Structure and bonding in amorphous $Cr_{1-x}C_x$ nanocomposite thin films: X-ray absorption spectra and first-principles calculations, J. Phys. Chem. C 120 (2016) 12890–12899, http://dx.doi.org/10.1021/acs.jpcc.6b03608.
[3] J.J. Rehr, Theoretical approaches to x-ray absorption fine structure, Rev. Mod. Phys. 72 (2000) 621–654, http://dx.doi.org/10.1103/RevModPhys.72.621.
[4] Y. Iwasawa, K. Asakura, M. Tada, XAFS Techniques for Catalysts, Nanomaterials, and Surfaces, Springer International Publishing, Cham, 2017, http://dx.doi.org/10.1007/978-3-319-43866-5.
[5] G. Bunker, Application of the ratio method of EXAFS analysis to disordered systems, Nucl. Instrum. Methods Phys. Res. 207 (1983) 437–444, http://dx.doi.org/10.1016/0167-5087(83)90655-5.
[6] P. Fornasini, F. Monti, A. Sanson, On the cumulant analysis of EXAFS in crystalline solids, J. Synchrotron Radiat. 8 (2001) 1214–1220, http://dx.doi.org/10.1107/S0909049501014923.
[7] P. Debye, Interferenz von Röntgenstrahlen und Wärmebewegung, Ann. Phys. 348 (1913) 49–92, http://dx.doi.org/10.1002/andp.19133480105.
[8] I. Waller, Zur Frage der Einwirkung der Wärmebewegung auf die Interferenz von Röntgenstrahlen, Z. Für Phys. 17 (1923) 398–408, http://dx.doi.org/10.1007/BF01328696.
[9] A. Sanson, On the neglecting of higher-order cumulants in EXAFS data analysis, J. Synchrotron Radiat. 16 (2009) 864–868, http://dx.doi.org/10.1107/S0909049509037716.
[10] P. Fornasini, S. a Beccara, G. Dalba, R. Grisenti, A. Sanson, M. Vaccari, F. Rocca, Extended x-ray-absorption fine-structure measurements of copper: local dynamics, anharmonicity, and thermal expansion, Phys. Rev. B 70 (2004) 174301, http://dx.doi.org/10.1103/PhysRevB.70.174301.
[11] T. Yokoyama, Path-integral effective-potential theory for EXAFS cumulants compared with the second-order perturbation, J. Synchrotron Radiat. 6 (1999) 323–325, http://dx.doi.org/10.1107/S0909049599001521.
[12] V.V. Hung, H.-K. Hieu, K. Masuda-Jindo, Study of EXAFS cumulants of crystals by the statistical moment method and anharmonic correlated Einstein model, Comput. Mater. Sci. 49 (2010), http://dx.doi.org/10.1016/j.commatsci.2010.02.005.
[13] G. Beni, P.M. Platzman, Temperature and polarization dependence of extended x-ray absorption fine-structure spectra, Phys. Rev. B 14 (1976) 1514–1518, http://dx.doi.org/10.1103/PhysRevB.14.1514.
[14] A.I. Frenkel, J.J. Rehr, Thermal expansion and x-ray-absorption fine-structure cumulants, Phys. Rev. B 48 (1993) 585–588, http://dx.doi.org/10.1103/PhysRevB.48.585.
[15] J. Freund, R. Ingalls, E.D. Crozier, Extended x-ray-absorption fine-structure study of copper under high pressure, Phys. Rev. B 43 (1991) 9894–9905, http://dx.doi.org/10.1103/PhysRevB.43.9894.
[16] T. Yokoyama, Y. Yonamoto, T. Ohta, A. Ugawa, Anharmonic interatomic potentials of octahedral Pt-halogen complexes studied by extended x-ray-absorption fine structure, Phys. Rev. B. Condens. Matter 54 (1996) 6921–6928, http://dx.doi.org/10.1103/physrevb.53.6111.
[17] N. Van Hung, J. Rehr, Anharmonic correlated einstein-model debye-waller factors, Phys. Rev. B 56 (1997) 43–46, http://dx.doi.org/10.1103/PhysRevB.56.43.
[18] N. Van Hung, N. Bao Trung, B. Kirchner, Anharmonic correlated Debye model Debye-Waller factors, Phys. B Condens. Matter 405 (2010) 2519–2525, http://dx.doi.org/10.1016/j.physb.2010.03.013.
[19] M.S. Daw, S.M. Foiles, M.I. Baskes, The embedded-atom method: a review of theory and applications, Mater. Sci. Rep. 9 (1993) 251–310, http://dx.doi.org/10.1016/0920-2307(93)90001-U.
[20] M.W. Finnis, J.E. Sinclair, A simple empirical N -body potential for transition metals, Philos. Mag. A 50 (1984) 45–55, http://dx.doi.org/10.1080/01418618408244210.
[21] V. Rosato, M. Guillope, B. Legrand, Thermodynamical and structural properties of f.c.c. transition metals using a simple tight-binding model, Philos. Mag. A 59

(1989) 321–336, http://dx.doi.org/10.1080/01418618908205062.
[22] A.P. Sutton, J. Chen, Long-range finnis-sinclair potentials, Philos. Mag. Lett. 61 (1990) 139–146, http://dx.doi.org/10.1080/09500839008206493.
[23] H. Rafii-Tabar, A.P. Sulton, Long-range Finnis-Sinclair potentials for f.c.c. metallic alloys, Philos. Mag. Lett. 63 (1991) 217–224, http://dx.doi.org/10.1080/09500839108205994.
[24] M.G. Newville, Local Thermodynamics Measurements of Dilute Binary Alloys Using XAFS, University of Washington, 1995.
[25] T. Comaschi, a Balerna, S. Mobilio, Thermal dependent anharmonicity effects on gold bulk studied by extended x-ray-absorption fine structure, J. Phys. Condens. Matter 21 (2009) 325404, http://dx.doi.org/10.1088/0953-8984/21/32/325404.
[26] M. Okube, A. Yoshiasa, O. Ohtaka, H. Fukui, Y. Katayama, W. Utsumi, Anharmonicity of gold under high-pressure and high-temperature, Solid State Commun. 121 (2002) 235–239, http://dx.doi.org/10.1016/S0038-1098(01)00494-X.
[27] J.J. Rehr, J.J. Kas, M.P. Prange, A.P. Sorini, Y. Takimoto, F. Vila, Ab initio theory and calculations of X-ray spectra, Comptes Rendus Phys. 10 (2009) 548–559, http://dx.doi.org/10.1016/j.crhy.2008.08.004.
[28] F. Cleri, V. Rosato, Tight-binding potentials for transition metals and alloys, Phys. Rev. B 48 (1993) 22–33, http://dx.doi.org/10.1103/PhysRevB.48.22.
[29] N.W. Ashcroft, N.D. Mermin, Solid State Physics, Harcourt College Publishers, 1976.
[30] S.I. Zabinsky, J.J. Rehr, A. Ankudinov, R.C. Albers, M.J. Eller, Multiple-scattering calculations of x-ray-absorption spectra, Phys. Rev. B 52 (1995) 2995–3009, http://dx.doi.org/10.1103/PhysRevB.52.2995.
[31] C. Kittel, Introduction to Solid State Physics, sixth ed., John-Wiley & Sons, Inc., New York, 1986.
[32] N.I. Papanicolaou, G.C. Kallinteris, G.A. Evangelakis, D.A. Papaconstantopoulos, M.J. Mehl, Second-moment interatomic potential for Cu-Au alloys based on total-energy calculations and its application to molecular-dynamics simulations, J. Phys. Condens. Matter 10 (1998) 10979, http://dx.doi.org/10.1088/0953-8984/10/48/018.
[33] A.A. Quong, First-principles determination of the interatomic-force-constant tensor of Au, Phys. Rev. B 49 (1994) 3226–3229, http://dx.doi.org/10.1103/PhysRevB.49.3226.
[34] V. Synecek, H. Chessin, M. Simerska, The temperature dependence of lattice vibrations in gold from X-ray diffraction measurements, Acta Crystallogr. Sect. A 26 (1970) 108–113, http://dx.doi.org/10.1107/S0567739470000141.
[35] J.W. Lynn, H.G. Smith, R.M. Nicklow, Lattice dynamics of gold, Phys. Rev. B 8 (1973) 3493–3499, http://dx.doi.org/10.1103/PhysRevB.8.3493.